Saturated Control of Time-Varying Formations and Trajectory Tracking for Unicycle Multi-agent Systems

D. Kostić, *Member*, *IEEE*, S. Adinandra, J. Caarls, N. van de Wouw, *Member*, *IEEE*,
and H. Nijmeijer, *Fellow*, *IEEE*

Abstract—We propose a synchronization approach to solve a problem where multiple unicycle agents are required to follow individual reference trajectories while maintaining a time-varying formation. Motions of the agents are synchronized thanks to coupling terms in their feedback control laws. Under saturation constraints on the control signals, our control laws guarantee global asymptotic zeroing of the synchronization errors and global asymptotic stability of the tracking error dynamics. For stronger controller couplings, the robustness of formation keeping to perturbations is increased. The proposed approach is successfully validated in experiments.

Index Terms—Tracking control, synchronization, formation control, control of non-holonomic systems, input saturation.

I. INTRODUCTION

FOR multiple nonholonomic agents (autonomous robots or vehicles), we propose a synchronization approach to solve a problem where the individual agents are required to follow predefined trajectories while keeping a desired spatial pattern (formation). Our algorithm applies to agents that feature nonholonomic kinematics of a unicycle [1]-[8] and need to maintain formations that can vary in time.

Formation control of multi-agent systems is actively studied in the field of cooperative control [3],[4]. Assignment of feasible formations, moving into a formation, maintenance of formation shape, and switching between formations are some examples of formation-control tasks. There are three approaches that are traditionally used for formation control, namely, the leader-follower strategy, the behavior-based approach, and the virtual structure approach.

The problem of formation control for unicycle-like agents is already addressed in the literature, see [2]-[8] and the references therein. Formation control with saturation constraints on control signals, as studied in [6], is less often in the literature, although such constraints are present in practice, hampering stability and performance of formation control. Control of time-varying formations of unicycles is rarely found in the literature; reference [2] is just an exception.

In our previous works [7] and [8], we have studied the

problem of motion coordination of unicycle agents. The scheme in [7] achieves coordination of two agents under certain excitation properties of the reference trajectories; no saturation constraints on the control signals are considered. The scheme in [8] relaxes the conditions on the excitation properties of the reference trajectories and achieves coordination of multiple agents under saturation constraints on the inputs. An algorithm for collision avoidance proposed in [8] is applicable with both control schemes.

In [7] and [8], the coordination is established by mutual coupling of motion controllers of the individual agents. These couplings are introduced at the level of the tracking errors. Although each scheme practically leads to some form of formation control, none is derived starting from some explicit formation control goal. The mathematical objective of both schemes is, in fact, trajectory tracking, so formation control is only an implicit consequence of mutual coupling of the tracking controllers of the interacting agents.

In this paper, we contribute a control design for multiple unicycle systems which guarantees formation control in addition to trajectory tracking. A systematic formation control design is the key advantage over [7] and [8]. Original contributions of this paper are: *i*) derivation of the general synchronization error dynamics for multiple unicycle systems, *ii*) a Lyapunov-based design of a saturated feedback controller for globally asymptotic stable trajectory tracking and globally asymptotic zeroing of the synchronization errors, *iii*) simultaneous trajectory tracking and control of time-varying formations where the linear and steering reference velocities of the individual agents can be mutually different, while the steering velocities can even be discontinuous, and *iv*) experimental verification.

Mathematical preliminaries are given in Section II. System dynamics are modeled in Section III. An algorithm for multi-agent trajectory tracking and formation control is derived in Section IV. Experimental results are shown in Section V. Conclusions are given in Section VI.

II. MATHEMATICAL PRELIMINARIES

From [8], we recall a lemma and class of saturation functions, as both are used in the control design in Section IV.

Lemma 1: Consider a scalar system:

$$\dot{x}(t) = -\phi(x(t)) + p(t), \qquad (1)$$

where ϕ and p are bounded and uniformly continuous functions of $x \in \mathbb{R}$ and $t \in \mathbb{R}$, respectively, such that $\phi(0) = 0$ and $x\phi(x) > 0$ if $x \neq 0$. If, for any $t_0 \geq 0$ and any initial condition $x(t_0)$, the solution $x(t)$ is bounded and

$\lim_{t\to\infty} x(t) = 0$, then

$$\lim_{t\to\infty} p(t) = 0. \tag{2}$$

Proof: See [3]. ∎

Like in [8], we define a class $\mathrm{BF}_{r,k}$ of uniformly continuous and bounded saturation functions indexed by (possibly time-variant) bounded parameters $r, k \in \mathrm{R}_+$:

$$\mathrm{BF}_{r,k} = \{\phi_r(kx): \mathbb{R} \to \mathbb{R} \mid \phi_r(kx) \text{ is uniformly continuous}$$
$$\text{and} -r \le \phi_r(kx) \le r \ \forall x \in \mathbb{R}\}. \tag{3}$$

A class $\mathrm{S}_{r,k}$ of functions within $\mathrm{BF}_{r,k}$ is considered here:

$$\mathrm{S}_{r,k} = \{\phi_r(kx): \mathbb{R} \to \mathbb{R} \mid \phi_r(kx) \in \mathrm{BF}_{r,k}, \phi_r(0) \equiv 0,$$
$$x\phi_r(kx) > 0 \text{ for all } x \neq 0, \phi_r(kx) + \phi_r(-kx) \equiv 0\}. \tag{4}$$

An example of a nontrivial, yet simple, function in $\mathrm{S}_{r,k}$ is:

$$\phi_r(kx) = r \tanh(kx). \tag{5}$$

III. PROBLEM FORMULATION AND SYSTEM MODELS

Here, we present a well-known model for unicycle systems and propose a model of synchronization between these systems. The models introduced here are used in Section IV for the purpose of control design.

A. Agent's Kinematics, Tracking and Coordination Errors, and Control Goal

We consider formation control of a group of n unicycle agents. The kinematics of an agent i ($i \in \{1,2,\dots,n\}$) is described by the following non-holonomic model [1]:

$$\begin{aligned} \dot{x}_i &= v_i\cos\theta_i, \\ \dot{y}_i &= v_i\sin\theta_i, \\ \dot{\theta}_i &= \omega_i, \end{aligned} \tag{6}$$

where v_i and ω_i are the linear and steering velocities, respectively, x_i and y_i are the planar coordinates of the agent in the world coordinate frame, and θ_i is the heading angle relative to the horizontal axis of the world frame. We define the following vectors of the state coordinates:

$$\mathbf{q}_i(t) = [x_i(t) \quad y_i(t)]^T, \tag{7}$$
$$\mathbf{p}_i(t) = [\mathbf{q}_i^T(t) \quad \theta_i(t)]^T. \tag{8}$$

The reference trajectory of agent i is given by:

$$\mathbf{p}_{r,i}(t) = \left[\mathbf{q}_{r,i}^T(t) \ \theta_{r,i}(t)\right]^T = \left[x_{r,i}(t) \ y_{r,i}(t) \ \theta_{r,i}(t)\right]^T. \tag{9}$$

Feasible reference trajectories satisfying the non-holonomic constraint in (6) should satisfy $-\dot{x}_{r,i}\sin\theta_{r,i}+\dot{y}_{r,i}\cos\theta_{r,i} = 0$. For $\dot{x}_{r,i} \neq 0$, $\dot{y}_{r,i} \neq 0$, the reference linear and steering velocities inducing the reference trajectory are given by

$$v_{r,i}(t) = \sqrt{\left(\dot{x}_{r,i}(t)\right)^2 + \left(\dot{y}_{r,i}(t)\right)^2},$$
$$\omega_{r,i}(t) = \left(\dot{x}_{r,i}(t)\ddot{y}_{r,i}(t) - \ddot{x}_{r,i}(t)\dot{y}_{r,i}(t)\right)/\left(v_{r,i}(t)\right)^2. \tag{10}$$

Now, the tracking errors are defined by:

$$\mathbf{e}_i(t) = \mathbf{q}_{r,i}(t) - \mathbf{q}_i(t), \tag{11a}$$

$$\theta_{e,i}(t) = \theta_{r,i}(t) - \theta_i(t). \tag{11b}$$

The reference trajectories define the desired spatial pattern of the agents (formation, such as a platoon). In this pattern, the Cartesian distances $(x_i - x_j, \ y_i - y_j)$, $i,j \in \{1,2,\dots,n\}$, $i \neq j$, of the agents change according the desired shape of the formation, which may vary in time according to:

$$\mathbf{q}_i(t) - \mathbf{q}_j(t) = \mathbf{q}_{r,i}(t) - \mathbf{q}_{r,j}(t). \tag{12}$$

Hence, the formation control objective is to let Cartesian tracking errors satisfy the following synchronization goal:

$$\mathbf{e}_i(t) \to \mathbf{e}_j(t) \text{ as } t \to \infty, \forall i,j \in \{1,2,\dots,n\}, \ i \neq j. \tag{13}$$

Motivated by [9], we define the position synchronization error as the difference between two tracking errors:

$$\boldsymbol{\varepsilon}_{i,j}(t)=\mathbf{e}_i(t) - \mathbf{e}_j(t), \ \ i,j \in \{1,2,\dots,n\}, \ i \neq j. \tag{14}$$

Since $\boldsymbol{\varepsilon}_{i,j} = -\boldsymbol{\varepsilon}_{j,i}$, to achieve the synchronization goal (13) it is sufficient to realize

$$\boldsymbol{\varepsilon}_{i,j} = \mathbf{0} \text{ for all } i \in \{1,\dots,n-1\} \text{ and } j \in \{i+1,\dots,n\}. \tag{15}$$

We point out that the synchronization goal (13) and its equivalent (15) do not per se require convergence of the individual Cartesian tracking errors $\mathbf{e}_i(t)$ to zero. In other words, the robots can maintain the desired formation (i.e. properties (13) and (15) can hold) even when each robot deviates from its own reference trajectory.

Our goal is to design control laws for v_i and ω_i in (6), $i \in \{1,2,\dots,n\}$, such that each agent asymptotically tracks its own reference trajectory $\mathbf{p}_{r,i}(t)$ while maintaining the prescribed spatial pattern (12). Moreover, if the motion of any of the agents is perturbed, then the control of the interacting agents should be coordinated such as to restore the formation (properties (13) and (15) are achieved) even at the cost of transient performance of tracking the individual trajectories.

B. Tracking and Coordination Errors Dynamics

For the control design, we consider Cartesian tracking errors of the agent i, $i \in \{1,2,\dots,n\}$, represented in its own coordinate frame [1]:

$$\mathbf{e}_{xy,i} = [x_{e,i} \quad y_{e,i}]^T = \mathbf{R}^T(\theta_i)\,\mathbf{e}_i, \tag{16}$$

where $\mathbf{R}(\theta_i)$ is the rotation matrix

$$\mathbf{R}(\theta_i) = \begin{bmatrix} \cos\theta_i & -\sin\theta_i \\ \sin\theta_i & \cos\theta_i \end{bmatrix}. \tag{17}$$

According to [1], the tracking error dynamics is given by:

$$\dot{\mathbf{e}}_{xy,i} = -\omega_i \mathbf{S}\mathbf{e}_{xy,i} + \begin{bmatrix} v_{r,i}\cos\theta_{e,i} - v_i \\ v_{r,i}\sin\theta_{e,i} \end{bmatrix}, \tag{18a}$$

$$\dot{\theta}_{e,i} = \omega_{r,i} - \omega_i, \tag{18b}$$

$$\mathbf{S} = \begin{bmatrix} 0 & -1 \\ 1 & 0 \end{bmatrix}. \tag{18c}$$

Considering the errors relative to the coordinate frame of the agent itself is convenient because of the appearance of the skew-symmetric matrix $\mathbf{S}$ in equation (18a). This matrix features several properties that facilitate control design using

Lyapunov functions that are quadratic in $\mathbf{e}_{xy,i}$. For the sake of the formation control design, we represent the coordination errors $\boldsymbol{\varepsilon}_{i,j}$ in the coordinate frame which is rotated about an angle $\theta_i + \theta_j$ relative to the world coordinate frame:

$$\boldsymbol{\sigma}_{i,j} = \mathbf{R}^T(\theta_i + \theta_j)\boldsymbol{\varepsilon}_{i,j}. \tag{19}$$

Clearly, $\boldsymbol{\sigma}_{i,j} = -\boldsymbol{\sigma}_{j,i}$ since $\boldsymbol{\varepsilon}_{i,j} = -\boldsymbol{\varepsilon}_{j,i}$. To derive dynamics of the errors $\boldsymbol{\sigma}_{i,j}$, we use the model (18a) and several well-known properties of the rotation matrix $\mathbf{R}(\theta_i)$ and the skew-symmetric matrix $\mathbf{S}$ defined by (17) and (18c), respectively:

$$\mathbf{R}(-\theta_i) = \mathbf{R}^T(\theta_i) = \mathbf{R}^{-1}(\theta_i), \tag{20a}$$
$$\mathbf{R}(\theta_i + \theta_j) = \mathbf{R}(\theta_i)\mathbf{R}(\theta_j), \tag{20b}$$
$$\dot{\mathbf{R}}(\theta_i(t)) = \frac{\mathrm{d}}{\mathrm{d}t}\mathbf{R}(\theta_i(t)) = \omega_i(t)\mathbf{S}\mathbf{R}(\theta_i(t)), \tag{20c}$$
$$\mathbf{S}^T = -\mathbf{S}, \tag{20d}$$
$$\mathbf{x}^T\mathbf{S}\mathbf{x} \equiv 0, \ \forall \mathbf{x} \in \mathbb{R}^2, \tag{20e}$$
$$\mathbf{S}\mathbf{R}(\theta_i) = \mathbf{R}(\theta_i)\mathbf{S}. \tag{20f}$$

From (14), (16), (19), and (20b) we can determine:

$$\boldsymbol{\sigma}_{i,j} = \mathbf{R}^T(\theta_j)\mathbf{R}^T(\theta_i)\big(\mathbf{R}(\theta_i)\mathbf{e}_{xy,i} - \mathbf{R}(\theta_j)\mathbf{e}_{xy,j}\big) =$$
$$= \mathbf{R}^T(\theta_j)\mathbf{e}_{xy,i} - \mathbf{R}^T(\theta_i)\mathbf{e}_{xy,j}. \tag{21}$$

The obtained relation between the tracking errors $\mathbf{e}_{xy,i}$, $\mathbf{e}_{xy,j}$ and the synchronization error $\boldsymbol{\sigma}_{i,j}$ facilitates the derivation of the synchronization error dynamics:

$$\dot{\boldsymbol{\sigma}}_{i,j} = \big(\omega_j\mathbf{S}\mathbf{R}(\theta_j(t))\big)^T \mathbf{e}_{xy,i} + \mathbf{R}^T(\theta_j)\Big(-\omega_i\mathbf{S}\mathbf{e}_{xy,i} +$$
$$\begin{bmatrix} v_{\mathrm{r},i}\cos\theta_{e,i} - v_i \\ v_{\mathrm{r},i}\sin\theta_{e,i} \end{bmatrix}\Big) - \big(\omega_i\mathbf{S}\mathbf{R}(\theta_i(t))\big)^T \mathbf{e}_{xy,j} -$$
$$\mathbf{R}^T(\theta_i)\Big(-\omega_j\mathbf{S}\mathbf{e}_{xy,j} + \begin{bmatrix} v_{\mathrm{r},j}\cos\theta_{e,j} - v_j \\ v_{\mathrm{r},j}\sin\theta_{e,j} \end{bmatrix}\Big)$$
$$= -(\omega_i + \omega_j)\mathbf{S}\big(\mathbf{R}^T(\theta_j)\mathbf{e}_{xy,i} - \mathbf{R}^T(\theta_i)\mathbf{e}_{xy,j}\big) +$$
$$\mathbf{R}^T(\theta_j)\begin{bmatrix} v_{\mathrm{r},i}\cos\theta_{e,i} - v_i \\ v_{\mathrm{r},i}\sin\theta_{e,i} \end{bmatrix} - \mathbf{R}^T(\theta_i)\begin{bmatrix} v_{\mathrm{r},j}\cos\theta_{e,j} - v_j \\ v_{\mathrm{r},j}\sin\theta_{e,j} \end{bmatrix}.$$

By substituting (21) into the last expression, we finalize the model of the synchronization error dynamics:

$$\dot{\boldsymbol{\sigma}}_{i,j} = -(\omega_i + \omega_j)\mathbf{S}\boldsymbol{\sigma}_{i,j} + \mathbf{R}^T(\theta_j)\begin{bmatrix} v_{\mathrm{r},i}\cos\theta_{e,i} - v_i \\ v_{\mathrm{r},i}\sin\theta_{e,i} \end{bmatrix}$$
$$-\mathbf{R}^T(\theta_i)\begin{bmatrix} v_{\mathrm{r},j}\cos\theta_{e,j} - v_j \\ v_{\mathrm{r},j}\sin\theta_{e,j} \end{bmatrix}. \tag{22}$$

The derived model features the same property as (18a): the skew-symmetric matrix $\mathbf{S}$ premultiplies the vector of states $\boldsymbol{\sigma}_{i,j}$. This property is a direct consequence of representing the synchronization error $\boldsymbol{\varepsilon}_{i,j}$ in the coordinate frame rotated about $\theta_i + \theta_j$ relative to the world frame. The appearance of the term $\mathbf{S}\boldsymbol{\sigma}_{i,j}$ in (22) encourages a Lyapunov-based design of a formation controller using a Lyapunov function candidate which is quadratic in $\boldsymbol{\sigma}_{i,j}$.

IV. CONTROL DESIGN

Here, we propose control laws for simultaneous trajectory tracking and formation control of n unicycle agents. In par-

ticular, we search for time-varying state-feedback control laws for $v_i(t)$ and $\omega_i(t)$, $i \in \{1,2,\dots,n\}$, that achieve global asymptotic stability of the tracking error dynamics (18) and global asymptotic convergence to zero of the synchronization errors whose dynamics are described by (22). We aim to achieve these goals under the input saturation constraints:

$$v_i(t) \le v_{\mathrm{max},i}, \ |\omega_i(t)| \le \omega_{\mathrm{max},i}, \ \forall t \ge 0. \tag{23}$$

Here, $v_{\mathrm{max},i}$ and $\omega_{\mathrm{max},i}$ are given positive constants. To solve this problem, we propose the following control law:

$$v_i(t) = v_{\mathrm{r},i}(t)\cos\theta_{e,i}(t) + \phi_{k_{\chi,i}(t)}\big(c_{\chi,i}\,\chi_i(t)\big), \tag{24a}$$
$$\omega_i(t) = \omega_{\mathrm{r},i}(t) + \phi_{k_{\theta,i}(t)}\big(c_{\theta,i}\,\theta_{e,i}(t)\big) +$$
$$v_{\mathrm{r},i}(t)\frac{\sin\theta_{e,i}(t)}{\theta_{e,i}(t)}\frac{kc_\gamma\,\gamma_i(t)}{\alpha(t)}, \tag{24b}$$

where χ_i, γ_i and α are the scalar functions defined by

$$[\chi_i(t) \quad \gamma_i(t)]^T = \mathbf{e}_{xy,i}(t) + \sum_{\substack{j=1 \\ j \ne i}}^{n} l_{i,j}\mathbf{R}(\theta_j(t))\boldsymbol{\sigma}_{i,j}(t), \tag{25}$$

$$\alpha(t) =$$
$$\sqrt{k^2 + \sum_{i=1}^{n}\mathbf{e}_{xy,i}^T(t)\mathbf{e}_{xy,i}(t) + \sum_{i=1}^{n-1}\sum_{j=i+1}^{n} l_{i,j}\boldsymbol{\sigma}_{i,j}^T(t)\,\boldsymbol{\sigma}_{i,j}(t)}. \tag{26}$$

Here, $k_{\chi,i}(t)$, $k_{\theta,i}(t)$, $c_{\chi,i}$, $c_{\theta,i}$, c_γ, k, and $l_{i,j}$ are the design parameters, while $\phi_{k_{\chi,i}}(c_{\chi,i}\chi)$ and $\phi_{k_{\theta,i}}(c_{\theta,i}\theta)$ are the saturation functions from the class $\mathrm{S}_{r,k}$ defined by (4). The parameters $k_{\chi,i}(t)$ and $k_{\theta,i}(t)$ define ranges of the corresponding saturation functions and both can be chosen as time-dependent. A rational behind time-dependency is explained at the end of this section. The parameters $c_{\chi,i}$, $c_{\theta,i}$ and c_γ are the gains of the control terms that take care of tracking the reference trajectories of the individual agents. The parameter $l_{i,j}$ is a coupling gain, and it appears in the control terms that take care of synchronization between the interacting agents, as defined by (13). The gain k normalizes the last term in (24b) to $[0, c_\gamma v_{\mathrm{r},i}(t)]$.

In this paper, we consider only the case where all interacting agents are mutually coupled with identical coupling gains, i.e. $l_{i,j} = l$, $l \ne 0$, $\forall i,j \in \{1,2,\dots,n\}$, $i \ne j$. It is not difficult to modify the control law (24) such as to cover scenarios with non-equal coupling gains including the coupling gains equal to zero (distributed control). Such scenarios will be studied in the future.

In the following theorem, we use Lyapunov stability theory to prove that the control law (24) leads to global asymptotic stability of the tracking error dynamics (18),(24) and global asymptotic convergence of the synchronization errors, obeying dynamics (22),(24), to zero under the input saturation constraints (23). Global asymptotic convergence of the synchronization errors implies realization of the synchronization goal formulated by (13).

Theorem 1: Consider a group of n unicycle agents with the kinematics of the agent i, $i \in \{1,2,\dots,n\}$, described by (6). Suppose that the reference trajectory of agent i is given

by (9), and this trajectory satisfies the non-holonomic constraint $-\dot{x}_{r,i}\sin\theta_{r,i}+\dot{y}_{r,i}\cos\theta_{r,i} = 0$. Consider the control laws (24a,b) with $v_{r,i}$ and $\omega_{r,i}$ as in (10) and the design parameters satisfying:

$$k_{\chi,i}(t), k_{\theta,i}(t), c_{\chi,i}, c_{\theta,i}, c_\gamma, k \in \mathbb{R}_+, \quad (27a)$$

$$l_{i,j} = l; \quad l \in \mathbb{R}_+, \quad (27b)$$

$$k_{\chi,i}(t) \leq v_{\max,i} - v_{r,i}(t), \quad (27c)$$

$$k_{\theta,i}(t) + c_\gamma v_{r,i}(t) \leq \omega_{\max,i} - |\omega_{r,i}(t)|, \quad (27d)$$

where $i,j \in \{1,2,\dots,n\}$, $i \neq j$, $t \in [0,\infty)$. Moreover, for all $i \in \{1,2,\dots,n\}$ we adopt the following assumptions:

- $v_{r,i}(t)$ is nonzero, bounded $\forall t \in [0,\infty)$, and uniformly continuous;
- $\omega_{r,i}(t)$ is bounded $\forall t \in [0,\infty)$;
- for given input constraints $v_{\max,i}, \omega_{\max,i} \in \mathbb{R}_+$, we have $|v_{r,i}(t)| < v_{\max,i}$ and $|\omega_{r,i}(t)| < \omega_{\max,i}$, $\forall t \in [0,\infty)$.

Then, the following two statements are valid:

1. the tracking error dynamics (18a,b) are globally asymptotically stable for all $i \in \{1,2,\dots,n\}$;
2. the synchronization errors $\boldsymbol{\sigma}_{i,j}(t)$ defined by (21) and satisfying dynamics (22) with $i,j \in \{1,2,\dots,n\}$, $i \neq j$, globally asymptotically converge to zero, i.e. $\lim_{t\to\infty} \boldsymbol{\sigma}_{i,j}(t) \to [0\ 0]^T$,

while the actuator constraints (23) are respected for all $i \in \{1,2,\dots,n\}$.

Proof: Consider a positive definite and proper Lyapunov function candidate:

$$V = kc_\gamma \sqrt{k^2 + \sum_{i=1}^{n} \mathbf{e}_{xy,i}^T \mathbf{e}_{xy,i} + \sum_{i=1}^{n-1} \sum_{j=i+1}^{n} l_{i,j} \boldsymbol{\sigma}_{i,j}^T \boldsymbol{\sigma}_{i,j}} +$$

$$0.5 \sum_{i=1}^{n} \theta_{e,i}^2 - k^2 c_\gamma, \quad (28)$$

where $k, c_\gamma, l_{i,j} \in \mathbb{R}_+$ are constant design parameters, $i,j \in \{1,2,\dots,n\}$, $i \neq j$. Having in mind (25), (26), by differentiating V along the solutions of the closed-loop system (18), (22), (24) with $i,j \in \{1,2,\dots,n\}$, $i \neq j$, we obtain

$$\frac{d}{dt}V = \frac{kc_\gamma}{\alpha}\left(\sum_{i=1}^{n} \mathbf{e}_{xy,i}^T \dot{\mathbf{e}}_{xy,i} + \sum_{i=1}^{n-1} \sum_{j=i+1}^{n} l_{i,j} \boldsymbol{\sigma}_{i,j}^T \dot{\boldsymbol{\sigma}}_{i,j}\right) + \sum_{i=1}^{n} \theta_{e,i} \dot{\theta}_{e,i}$$

$$= \frac{kc_\gamma}{\alpha}\sum_{i=1}^{n} \mathbf{e}_{xy,i}^T \left(-\omega_i \mathbf{S}\mathbf{e}_{xy,i} + \begin{bmatrix} v_{r,i}\cos\theta_{e,i} - v_i \\ v_{r,i}\sin\theta_{e,i} \end{bmatrix}\right) +$$

$$\frac{kc_\gamma}{\alpha}\sum_{i=1}^{n-1} \sum_{j=i+1}^{n} l_{i,j} \boldsymbol{\sigma}_{i,j}^T \left(-(\omega_i + \omega_j)\mathbf{S}\boldsymbol{\sigma}_{i,j} + \right.$$

$$\left. \mathbf{R}^T(\theta_j)\begin{bmatrix} v_{r,i}\cos\theta_{e,i} - v_i \\ v_{r,i}\sin\theta_{e,i} \end{bmatrix} - \mathbf{R}^T(\theta_i)\begin{bmatrix} v_{r,j}\cos\theta_{e,j} - v_j \\ v_{r,j}\sin\theta_{e,j} \end{bmatrix}\right)$$

$$+ \sum_{i=1}^{n} \theta_{e,i}(\omega_{r,i} - \omega_i)$$

$$= \frac{kc_\gamma}{\alpha}\sum_{i=1}^{n} \left(\mathbf{e}_{xy,i}^T + \sum_{\substack{j=1 \\ j\neq i}}^{n} l_{i,j} \boldsymbol{\sigma}_{i,j}^T \mathbf{R}^T(\theta_j)\right)\begin{bmatrix} v_{r,i}\cos\theta_{e,i} - v_i \\ v_{r,i}\sin\theta_{e,i} \end{bmatrix}$$

$$+ \sum_{i=1}^{n} \theta_{e,i}(\omega_{r,i} - \omega_i)$$

$$= \frac{kc_\gamma}{\alpha}\sum_{i=1}^{n} [\chi_i \quad \gamma_i]\begin{bmatrix} -\phi_{k_{\chi,i}}(c_{\chi,i}\,\chi_i) \\ v_{r,i}\sin\theta_{e,i} \end{bmatrix}$$

$$+ \sum_{i=1}^{n} \theta_{e,i}\left(-\phi_{k_{\theta,i}}(c_{\theta,i}\,\theta_{e,i}) - v_{r,i}\frac{\sin\theta_{e,i}}{\theta_{e,i}}\frac{kc_\gamma\,\gamma_i}{\alpha}\right)$$

$$= -\sum_{i=1}^{n}\left(\frac{kc_\gamma}{\alpha}\chi_i\phi_{k_{\chi,i}}(c_{\chi,i}\chi_i) + \theta_{e,i}\phi_{k_{\theta,i}}(c_{\theta,i}\theta_{e,i})\right) \leq 0, \quad (29)$$

where we used (20e) and (27b). The last inequality in (29), which follows from properties of functions $\phi_{k_{\chi,i}}$, $\phi_{k_{\theta,i}}$ from the class $S_{r,k}$ defined by (4), implies that the tracking error dynamics in (18), in terms of the tracking errors $x_{e,i}(t)$, $y_{e,i}(t)$, $\theta_{e,i}(t)$, $i \in \{1,2,\dots,n\}$, are stable. By virtue of (21), the synchronization errors $\boldsymbol{\sigma}_{i,j}$ are uniformly bounded for all $i,j \in \{1,2,\dots,n\}$, $i \neq j$, over $t \in [0,\infty)$. It remains to prove the global asymptotic convergence of both the tracking and synchronization errors to zero.

From the last inequality in (29), we can determine

$$0 \geq \int_0^\infty dV(t) \geq -\sum_{i=1}^{n}\left\{kc_\gamma \int_0^\infty \chi_i(t)\phi_{k_{\chi,i}(t)}(c_{\chi,i}\chi_i(t))dt \right.$$

$$\left. + \int_0^\infty \theta_{e,i}(t)\phi_{k_{\theta,i}(t)}(c_{\theta,i}\theta_{e,i}(t))dt\right\}, \quad (30)$$

which, having in mind that V is nonnegative (i.e. lower bounded by zero), implies that the integrals at the right-hand side in (30) exist and are finite. Since by definition (4), both $\chi_i(t)\phi_{k_{\chi,i}(t)}(c_{\chi,i}\chi_i(t))$ and $\theta_{e,i}(t)\phi_{k_{\theta,i}(t)}(c_{\theta,i}\theta_{e,i}(t))$ are non-negative, then for all $i,j \in \{1,2,\dots,n\}$, $i \neq j$, we have $\chi_i\phi_{k_{\chi,i}}(c_{\chi,i}\chi_i) \in L_1(0,\infty)$ and $\theta_{e,i}\phi_{k_{\theta,i}}(c_{\theta,i}\theta_{e,i}) \in L_1(0,\infty)$. Since

- $x_{e,i}(t)$, $y_{e,i}(t)$ and $\theta_{e,i}(t)$ are solutions of the continuous error dynamics (18a,b),
- $\boldsymbol{\sigma}_{i,j}(t)$ is solution of the continuous error dynamics (22),
- $\theta_i(t)$ is solution of the continuous system (6),
- $\chi_i(t)$ and $\gamma_i(t)$ are continuous functions of $x_{e,i}(t)$, $y_{e,i}(t)$, $\boldsymbol{\sigma}_{i,j}(t)$ and $\theta_j(t)$ according to (25),
- $\phi_r(kx)$ is by assumption uniformly continuous over $t \in [0,\infty)$,
- the systems (6), (18a,b) and (22) are all excited with control inputs (24a,b) depending on uniformly continuous functions $\chi_i(t)$, $\gamma_i(t)$, $\theta_{e,i}(t)$ and bounded functions $v_{r,i}(t)$ and $\omega_{r,i}(t)$,

we can conclude that for all $i \in \{1,2,\dots,n\}$ $\chi_i(t)\phi_{k_{\chi,i}(t)}(c_{\chi,i}\chi_i(t))$ and $\theta_{e,i}(t)\phi_{k_{\theta,i}(t)}(c_{\theta,i}\theta_{e,i}(t))$ must be uniformly continuous over $t \in [0,\infty)$. With the help of Barbălat's lemma [10], we get

$$\lim_{t\to\infty} \sum_{i=1}^{n}\left[\chi_i(t)\phi_{k_{\chi,i}(t)}(c_{\chi,i}\chi_i(t)) \right.$$

$$\left. + \theta_{e,i}(t)\phi_{k_{\theta,i}(t)}(c_{\theta,i}\theta_{e,i}(t))\right] = 0, \quad (31)$$

implying

$$\lim_{t\to\infty}[|\chi_i(t)| + |\theta_{e,i}(t)|] = 0, \ \forall i \in \{1,2,\dots,n\}. \quad (32)$$

It remains to prove

$$\lim_{t\to\infty} \mathbf{e}_{xy,i}(t) = \mathbf{0}_2 = \begin{bmatrix} 0 \\ 0 \end{bmatrix}, \ \forall i \in \{1,2,\dots,n\}, \quad (33)$$

which will, according to (21), imply

$$\lim_{t\to\infty} \boldsymbol{\sigma}_{i,j}(t) = \mathbf{0}_2, \ \forall i,j \in \{1,2,\dots,n\}, i \neq j. \quad (34)$$

From the closed-loop system (18b), (24b) we obtain:

$$\dot{\theta}_{e,i}(t) = -\phi_{k_{\theta,i}(t)}\big(c_{\theta,i}\theta_{e,i}(t)\big) - \frac{\sin\theta_{e,i}(t)}{\theta_{e,i}(t)}\frac{v_{r,i}(t)kc_\gamma\gamma_i(t)}{\alpha(t)}. \quad (35)$$

Since (32) implies $\lim_{t\to\infty}\theta_{e,i}(t) = 0$, a direct application of the Lemma 1 to (35) results in:

$$\lim_{t\to\infty}\frac{\sin\theta_{e,i}(t)}{\theta_{e,i}(t)}\frac{v_{r,i}(t)kc_\gamma\gamma_i(t)}{\alpha(t)} = 0. \quad (36)$$

Since in the theorem every $v_{r,i}(t)$ is assumed to be nonzero $\forall t \in [0,\infty)$, and using the fact that $0 < \alpha(t) < \infty$ for all $t \in [0,\infty)$, we can conclude that

$$\lim_{t\to\infty}\gamma_i(t) = 0, \ \ \forall i \in \{1,2,\dots,n\}. \quad (37)$$

Note that expressions (31) and (35) do not depend on $\omega_{r,i}(t)$. Consequently, uniform continuity of $\omega_{r,i}(t)$ is not required to guarantee (34) and (37).

From (25), (32) and (37), we find for all $i \in \{1,2,\dots,n\}$:

$$\lim_{t\to\infty}\Big(\mathbf{e}_{xy,i}(t) + \sum_{\substack{j=1\\j\neq i}}^{n} l_{i,j}\mathbf{R}\big(\theta_j(t)\big)\boldsymbol{\sigma}_{i,j}(t)\Big) = \mathbf{0}_2. \quad (38)$$

If we insert expression (21) into (38) and apply properties (20a) and (20b), we obtain:

$$\lim_{t\to\infty}\Big[\Big(1 + \sum_{\substack{j=1\\j\neq i}}^{n} l_{i,j}\Big)\mathbf{e}_{xy,i}(t) -$$

$$\sum_{\substack{j=1\\j\neq i}}^{n} l_{i,j}\mathbf{R}\big(\theta_j(t) - \theta_i(t)\big)\mathbf{e}_{xy,j}(t)\Big] = \mathbf{0}_2. \quad (39)$$

Having in mind assumption (27b), we can define gain p as:

$$p = \frac{l_{i,j}}{1 + \sum_{\substack{j=1\\j\neq i}}^{n} l_{i,j}} = \frac{l}{1 + (n-1)l} = \frac{1}{\frac{1}{l} + n - 1}. \quad (40)$$

Since a multi-agent system implies $n \geq 2$, and since according to (27b) we have $l > 0$, then the following is guaranteed:

$$p \neq \frac{1}{n-1} \ \text{ and } \ p > 0. \quad (41)$$

Now, we can rewrite (39) as follows:

$$\lim_{t\to\infty}\Big(\mathbf{e}_{xy,i}(t) - p\sum_{\substack{j=1\\j\neq i}}^{n}\mathbf{R}\big(\theta_j(t) - \theta_i(t)\big)\mathbf{e}_{xy,j}(t)\Big) = \mathbf{0}_2.$$

By taking all $i \in \{1,2,\dots,n\}$ into account, we can rewrite the previous expression as follows:

$$\lim_{t\to\infty}\Big(\mathbf{M}_n(t)\mathbf{e}_{xy}(t)\Big) = \mathbf{0}_{2n}, \quad (42)$$

where $\mathbf{M}_n \in \mathbb{R}^{2n\times 2n}$ is a square symmetric matrix given by

$$\mathbf{M}_n(\theta_1, \theta_2, \dots, \theta_n) =$$
$$\begin{bmatrix} \mathbf{I}_2 & -p\mathbf{R}^T(\theta_1-\theta_2) & \cdots & -p\mathbf{R}^T(\theta_1-\theta_n) \\ -p\mathbf{R}(\theta_1-\theta_2) & \mathbf{I}_2 & \cdots & -p\mathbf{R}^T(\theta_2-\theta_n) \\ \vdots & \vdots & \ddots & \vdots \\ -p\mathbf{R}(\theta_1-\theta_n) & -p\mathbf{R}(\theta_2-\theta_n) & \cdots & \mathbf{I}_2 \end{bmatrix},$$
$$(43)$$

$$\mathbf{e}_{xy} = \begin{bmatrix} \mathbf{e}_{xy,1}^T & \mathbf{e}_{xy,2}^T & \cdots & \mathbf{e}_{xy,n}^T \end{bmatrix}^T. \quad (44)$$

Although $\mathbf{M}_n$ depends on $\theta_1, \dots \theta_n$, its determinant is always constant:

$$det(\mathbf{M}_n) = (n-1)^2\Big(p - \frac{1}{n-1}\Big)^2(p+1)^{2(n-1)}. \quad (45)$$

Expression (45) is derived from (43) by means of mathematical induction, starting from $n = 2$, using the well-known property (46) for matrices $\mathbf{A} \in \mathbb{R}^{n\times n}$, $\mathbf{B} \in \mathbb{R}^{n\times m}$, $\mathbf{C} \in \mathbb{R}^{m\times n}$, $\mathbf{D} \in \mathbb{R}^{m\times m}$ with $det(\mathbf{D}) \neq 0$:

$$det\Big(\begin{bmatrix} \mathbf{A} & \mathbf{B} \\ \mathbf{C} & \mathbf{D} \end{bmatrix}\Big) = det(\mathbf{D})det(\mathbf{A} - \mathbf{B}\mathbf{D}^{-1}\mathbf{C}). \quad (46)$$

Having in mind (41), in other words that all coupling gains $l_{i,j}$ satisfy (27b), from (45) we conclude that $det(\mathbf{M}_n) \neq 0$ for $n \geq 2$. Then, from (42) it follows that property (33) must hold. Consequently, property (34) is also satisfied. By virtue of (14), (15) and (19), the fulfillment of property (34) implies achievement of the synchronization objective (13).

Selection of the design parameters according to (27c,d) trivially ensures that the control inputs (24a,b) fulfill (23). ∎

We point out that our control design leads to globally asymptotically stable trajectory tracking error dynamics and the global asymptotic convergence of the synchronization errors to zero, even if $\omega_{r,i}(t)$ is discontinuous (yet bounded).

The design parameters in (24a,b) offer high freedom in tuning the transient behavior of the closed-loop system. During periods of slower movements, we can allow high-gain feedback by increasing the time-varying parameters $k_{\chi,i}$ and $k_{\theta,i}$, without violating the constraints (23). Higher gains can improve the tracking performance at low velocities, especially if an agent is subject to disturbances (e.g., friction on the robot wheels, noise in the feedback signals). If the individual agents suffer from perturbations, by means of the strictly positive coupling gain l, see (27b), the controller (24a,b) mediates between tracking of the reference trajectories of the individual agents and keeping of the formation. Higher l increases interactions among the agents and improves robustness of the formation keeping against perturbations. This will be illustrated in the next section.

V. Experimental Case-study

To illustrate the results presented so far, we conduct experiments using four mobile robots (model E-puck [11]). The reference trajectories $\mathbf{p}_{r,i}(t)$, $i \in \{1,2,3,4\}$, are chosen such that the robots form a platoon-like formation. The platoon of robots makes a round trip along an ellipse. The desired mutual Cartesian distances $(x_{r,i} - x_{r,j}, y_{r,i} - y_{r,j})$, $i,j \in \{1,2,\dots,n\}$, $i \neq j$, vary in time along an ellipse. The reference robot paths are depicted in Fig. 1 with the solid lines.

For $i,j \in \{1,2,3,4\}$, $i \neq j$, we use $v_{max,i} = 0.1$ m/s, $\omega_{max,i} = 1.7$ rad/s and the controller (24a,b) with the saturation function defined by (5b), $c_{\chi,i} = c_\gamma = k = 10$, $c_{\theta,i} = 1$, $k_{\chi,i}(t) = v_{max,i} - v_{r,i}(t)$, $k_{\theta,i} = 0.4$, and $l_{i,j} = l = 2$. Time-varying feedback gain $k_{\chi,i}(t)$ is higher at lower velocities, which increases robustness against disturbances (e.g. friction) at these velocities without violating the constraints in (23). The design parameters are tuned such as to

demonstrate that in the absence of perturbations four robots asymptotically track their own reference trajectories, while, if subject to perturbations, the robots prefer to maintain the prescribed formation at the cost of the tracking performance. The emphasis on formation keeping is achieved by choosing a relatively strong coupling coefficient of $l = 2$.
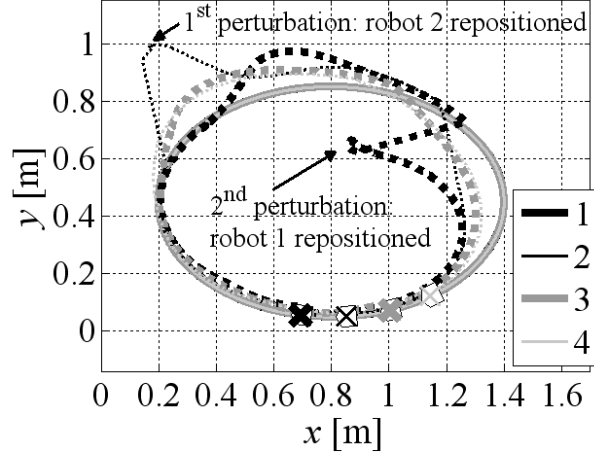

Fig. 1. Reference (solid) and actual (dotted) robot paths in the experiment; the initial and terminal positions are coinciding and are indicated with '×'.

To practically verify formation keeping, during the experiment we manually perturbed the formation two times, by repositioning robots 2 and 1 at time instants 20 s and 41 s, respectively. The actual robot paths are depicted in Fig. 2 by the dotted lines. Each time a robot is repositioned, the other ones start moving away from their reference trajectories aiming to restore the prescribed platoon-like formation. After recovering the formation, the robots continue tracking their own reference trajectories. As an illustration, in Fig. 2 we show the tracking errors defined by (11a,b) together with errors in keeping the formation $\boldsymbol{\delta}_{i,j}(t) = \Delta_{\mathrm{r},i,j}(t) - \Delta_{i,j}(t)$.
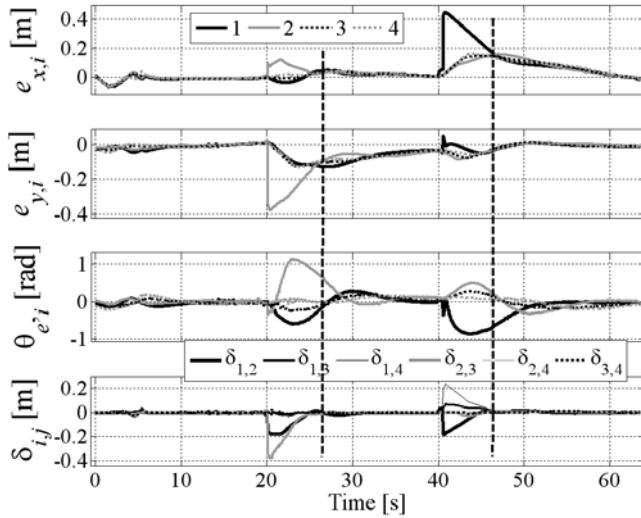

Fig. 2. Experimentally measured tracking errors ($e_{x,i}$, $e_{y,i}$, $e_{\theta,i}$) and errors in keeping the formation $\delta_{i,j}$; the vertical dashed lines identify finishing of transients of the formation errors.

Here, $\Delta_{\mathrm{r},i,j}$ and $\Delta_{i,j}$ are the reference and actual Euclidean distances between robots i and j, respectively:

$$\Delta_{i,j}(t) = \sqrt{\left(\mathbf{q}_i(t) - \mathbf{q}_j(t)\right)^T \left(\mathbf{q}_i(t) - \mathbf{q}_j(t)\right)}, \quad (47)$$

$i,j \in \{1,2,3,4\}$, $i \neq j$. A closer inspection of Fig. 2 confirms that the transients of the formation errors are faster than the transients of the tracking errors: after perturbations, the robots first restore the desired formation and then converge to their reference trajectories. This property is gained by introducing the synchronization errors in the control law (24a,b). If formation keeping is more important than tracking the reference trajectories of the individual robots , then a higher value of the coupling gain l is needed; a lower value of l is used if the trajectory tracking has the priority.

VI. CONCLUSIONS

We propose a synchronization approach to formation control of multiple nonholonomic agents. In addition to tracking their own reference trajectories, the interacting agents synchronize their motions such as to maintain the desired time-varying formation. We define synchronization errors as difference position errors between every pair of the interacting agents and derive a model describing the synchronization error dynamics. This model facilitates a Lyapunov-based design of the synchronization controller. Herewith, we derive a controller which leads to global asymptotic stability of the tracking errors dynamics and global asymptotic convergence of the synchronization errors to zero, under saturation constraints on the control inputs of the individual agents. The reference linear and steering velocities of the individual agents can all be different, while the steering velocities can even be discontinuous. Experimental results verify quality of the proposed approach.

REFERENCES

[1] Y. Kanayama, Y. Kimura, F. Miyazaki, T. Noguchi, "A Stable Tracking Control Method for an Autonomous Mobile Robot," *IEEE Conf. Rob. Automat.*, pp. 384–389, Cincinnati, OH, 1990.

[2] E.W. Justh, P.S. Krishnaprasad, "Equilibria and Steering Laws for Planar Formations," *Sys. Contr. Lett.*, Vol. 52, No. 1, pp. 25-38, 2004.

[3] Y.Q. Chen, Z. Wang, "Formation Control: a Review and a New Consideration," *IEEE/RSJ Int. Conf. Int. Robots and Systems*, pp. 3181-3186, Alberta, Canada, 2005.

[4] K.Y. Pettersen, J.T. Gravdahl, H. Nijmeijer, Eds. *Group Coordination and Cooperative Control*. Springer-Verlag, London, 2006.

[5] C. Yoshioka, T. Namerikawa, "Formation Control of Nonholonomic Multi-vehicle Systems Based on Virtual Structure," *17th IFAC World Congress*, pp. 5149-5154, 2008.

[6] L. Consolini, F. Morbidi, D. Prattichizzo, M. Tosques, "Stabilization of a Hierarchical Formation of Unicycle Robots with Velocity and Curvature Constraints," *IEEE Trans. on Robotics*, Vol. 25, No. 5, pp. 1176-1184, 2009.

[7] T.H.A. van den Broek, N. van de Wouw, H. Nijmeijer, "Formation Control of Unicycle Mobile Robots: a Virtual Structure Approach," *IEEE Conf. Dec. Control*, pp. 3264-3269, Shanghai, China, 2009.

[8] D. Kostić, S. Adinandra, J. Caarls, H. Nijmeijer, "Collision-free Motion Coordination of Unicycle Multi-agent Systems," *American Control Conf.*, pp. 3186-3191, Baltimore, USA, 2010.

[9] D. Sun, C. Wang, W. Shang, G. Feng, "A Synchronization Approach to Trajectory Tracking of Multiple Mobile Robots While Maintaining Time-Varying Formations," *IEEE Trans. on Robotics*, Vol. 25, No. 5, pp. 1074-1086, 2009.

[10] V.M. Popov, *Hyperstability of Control Systems*, Springer-Verlag, Berlin, 1973.

[11] F. Mondada, M. Bonani, *E-puck education robot*, www.e-puck.org